Supporting Material for:

A novel microfluidic device integrating focus-separation speed reduction design and trap arrays for high-throughput capture of circulating tumor cells †

Chunyang Lu [1§], Jian Xu [2§], Jintao Han [1], Xiao Li [3], Ningtao Xue [4], Jinsong Li [4], Wenhua Wu [4], Xinlei Sun [5], Yugang Wang [1], Qi Ouyang [2, 3, 6], Gen Yang [1*], Chunxiong Luo [2, 3*]

[1] State Key Laboratory of Nuclear Physics and Technology, School of Physics, Peking University, Beijing 100871, China;

[2] The State Key Laboratory for Artificial Microstructures and Mesoscopic Physics, School of Physics, Peking University, Beijing 100871, China;

[3] Center for Quantitative Biology, Academy for Advanced Interdisciplinary Studies, Peking University, Beijing 100871, China;

[4] Jining No. 2 People's Hospital, Jining 272049, China;

[5] Jining Tumor Hospital, Jining 272007, China;

[6] Peking-Tsinghua Center for Life Sciences, Peking University, Beijing 100871, China.

[§] Co-first authors

* To whom correspondence should be addressed: Gen Yang, Email: gen.yang@pku.edu.cn; Chunxiong Luo, Email: pkuluocx@pku.edu.cn.

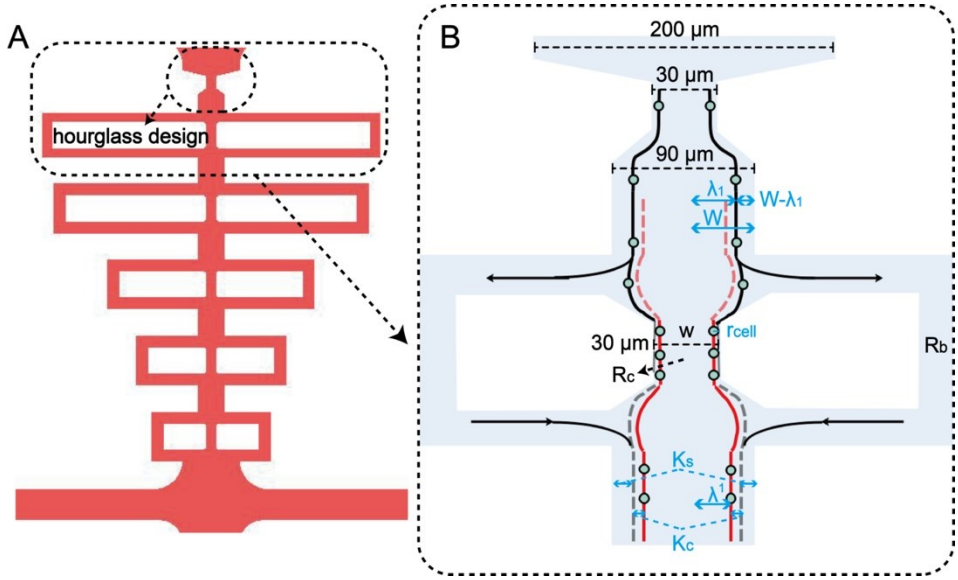

Supplementary Figure 1: Schematic diagram of the focus effect. (**A**) The design of a group of focus-separation apparatus. (**B**) An enlarged view of the first focus structure. R_c is the flow resistance of the central channel, and R_b is the flow resistance of the branch channel, r_{cell} is CTC radius, w is the width of the central channel, and W is half the width of the central channel.

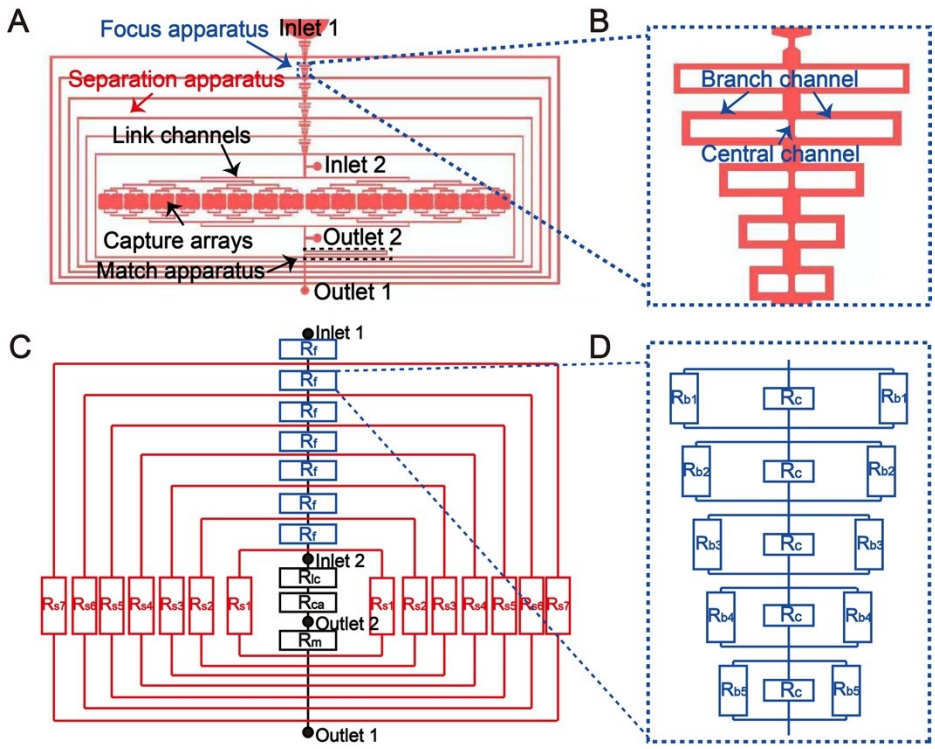

Supplementary Figure 2: Design and flow resistances of the microfluidic device. (**A**) The overall design of the microfluidic device. (**B**) An enlarged view of the focus apparatus from A. (**C**) All R (flow resistances) of each apparatus are shown in the circuit diagram. R_f is the flow resistance of the focus apparatus, R_{s1} to R_{s7} are the flow resistances from the seven separations, R_{lc} is the flow resistance of the link channels, R_{ca} is the flow resistance of the capture arrays, and R_m is the flow resistance of the match apparatus. (**D**) An enlarged view of the circuit diagram of the focus apparatus. R_c is the flow resistance of the central channel, and R_{b1} to R_{b5} are the flow resistances of the branch channels.

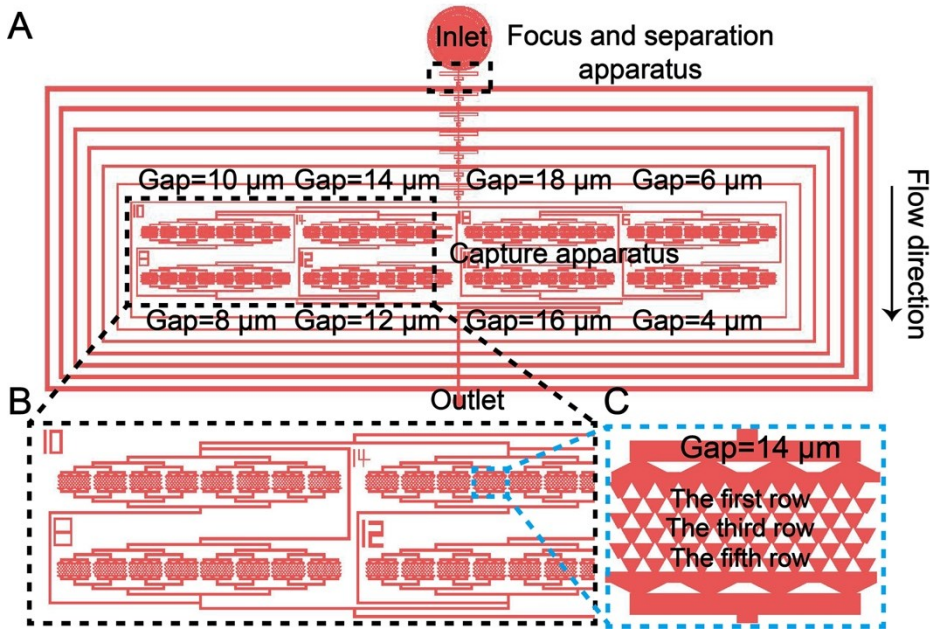

Supplementary Figure 3: The design of the 8-gap chip. (**A**) The overview of the face of the 8-gap chip: the 8 gaps included 4, 6, 8, 10, 12, 14, 16, and 18 μm, and the 8 capture apparatuses were independent and in parallel. (**B**) The enlarged view of the capture apparatus. (**C**) A further enlarged view of the capture apparatus, including 6 rows of triangular prisms, which formed 5 rows of capture gaps.

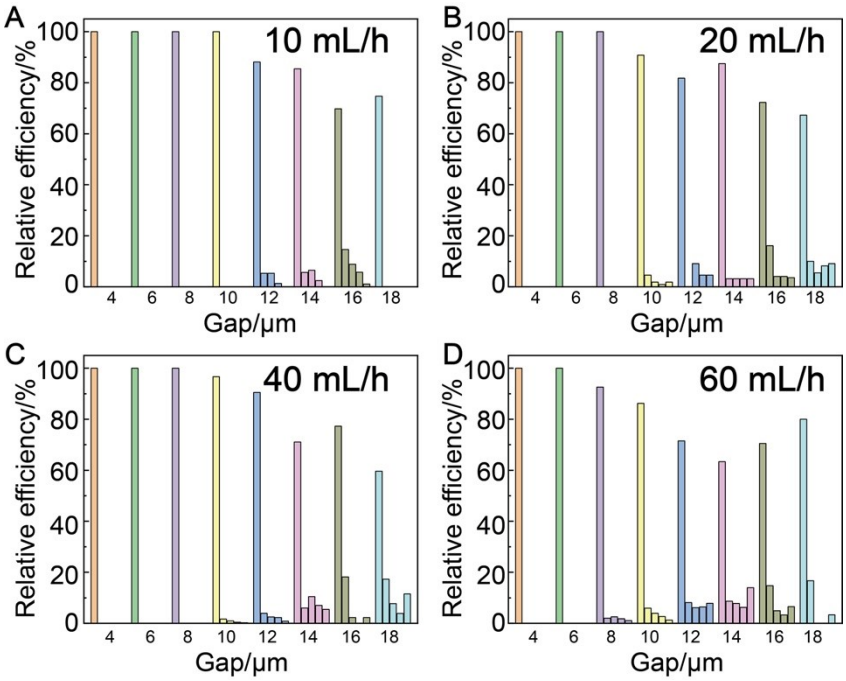

Supplementary Figure 4: Cancer cell distribution among 8 different gaps in the 8-gap chip under 4 different flow rates: (**A**) 10 mL/h; (**B**) 20 mL/h; (**C**) 40 mL/h; (**D**) 60 mL/h. Eight different gaps are shown in different colors. For each gap, there were five columns from left to right, representing the first to fifth rows of capture gaps, respectively.

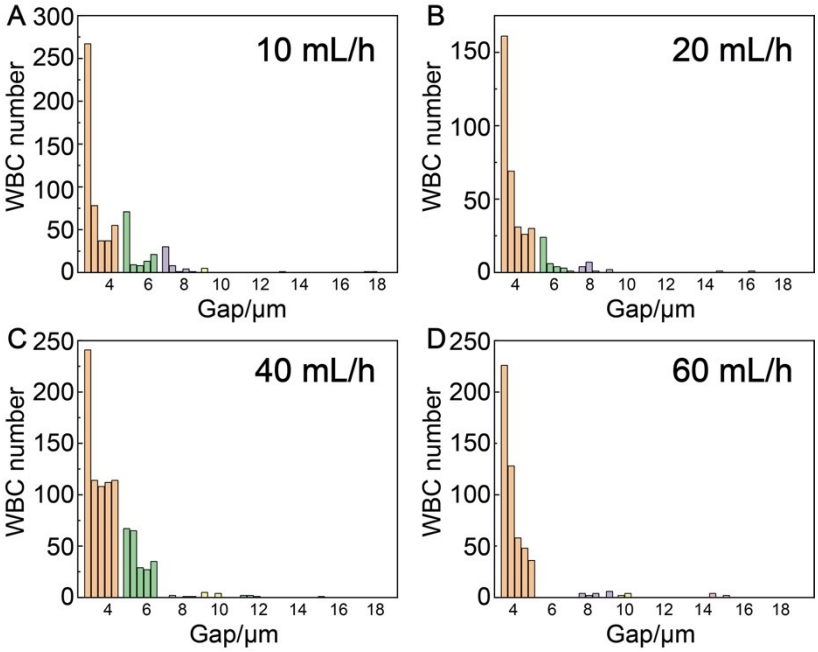

Supplementary Figure 5: Captured WBC distribution among 8 different gaps in the 8-gap chip under 4 different flow rates: (**A**) 10 mL/h; (**B**) 20 mL/h; (**C**) 40 mL/h; (**D**) 60 mL/h. Eight different gaps are shown in different colors. For each gap, there were five columns from left to right, representing the first to fifth rows of capture gaps, respectively. From the results of Supplementary Fig. S3 and S4, we chose 8 μm as the minimum gap in the final design to ensure that the arrays can capture all the CTCs but allow most of the WBCs to pass through.

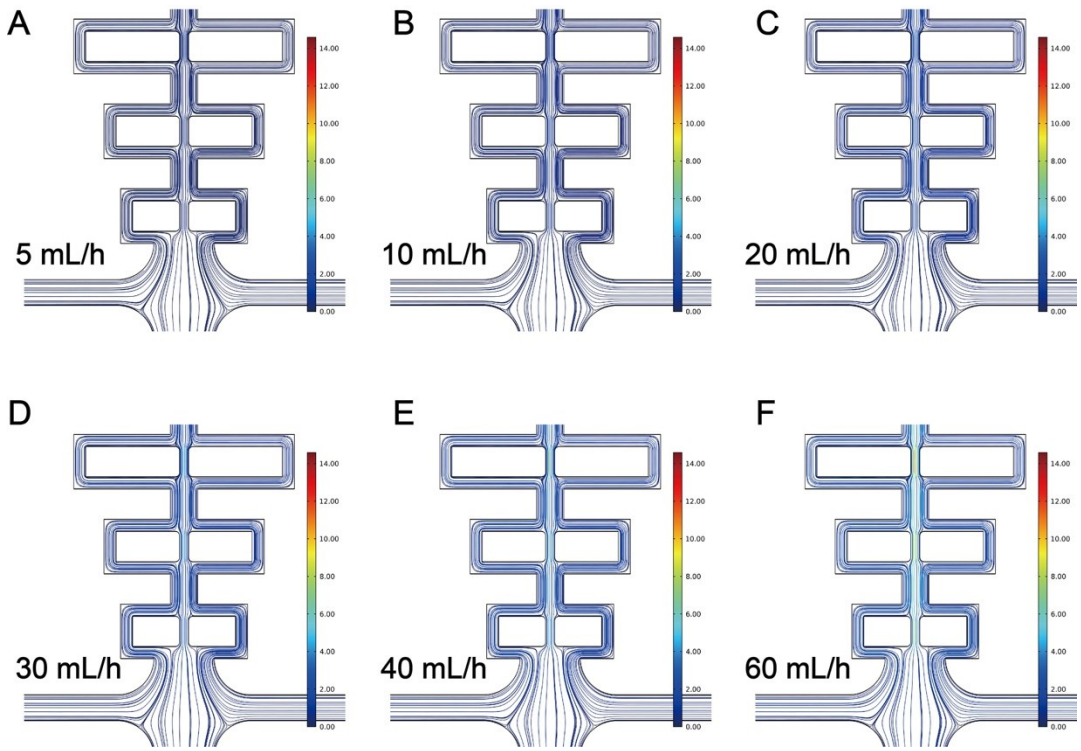

Supplementary Figure 6: The streamlines of the first focus-separation apparatus under 5, 10, 20, 30, 40 and 60 mL/h.

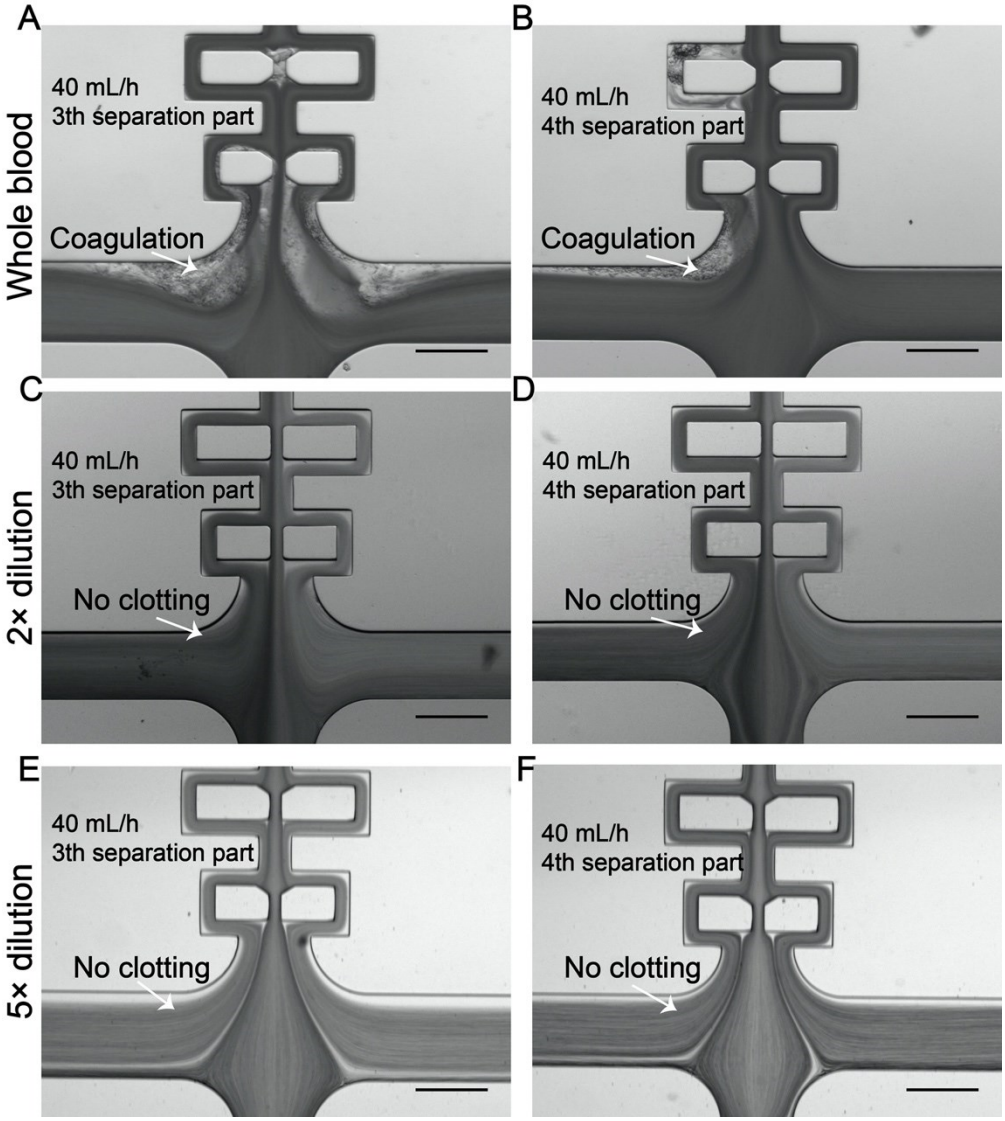

Supplementary Figure 7: Different diluted blood samples in the chip. (**A**, **B**) The blood coagulated without being diluted. (**C** to **F**) There is no coagulation while using 2× and 5× diluted blood. (Scale bars: 200 μm.) Therefore, we chose 2× diluted blood and 40 mL/h as the final experimental conditions to prevent blood clotting and achieve a high throughput and high capture efficiency at the same time.

Table S1. The design parameters of the channels in the chip.

Focus apparatus		**Length/μm**	**Width/μm**	**Height/μm**	**Normalized flow resistance (R)**
The first focus structure	The central channel	100	30	60	1
	The branch channel	1200	30	60	12
The second focus structure	The central channel	100	30	60	1
	The branch channel	1100	40	60	5.73
The third focus structure	The central channel	100	30	60	1
	The branch channel	720	40	60	3.75
The fourth focus structure	The central channel	100	30	60	1
	The branch channel	520	40	60	2.71
The fifth focus structure	The central channel	100	30	60	1
	The branch channel	410	40	60	2.14
Separation apparatus	**Length/μm**	**Width/μm**	**Height/μm**	**Normalized flow resistance (R)**	**R of the inner part of the separation channels**
The first separation	72552	220	60	17.8	8.76
The second separation	68170	200	60	19.3	9.18
The third separation	63874	180	60	21.3	9.79
The fourth separation	59658	160	60	24	10.8
The fifth separation	55532	140	60	27.8	13
The sixth separation	51406	110	60	38.7	16.6
The seventh separation	47280	90	60	56.8	22.1
Capture apparatus	**Equivalent length/μm**	**Width/μm**	**Height/μm**	**Normalized flow resistance (R)**	
Link channels	15100	120	60	9.47	
Capture arrays	N/A	N/A	60	0.0538	
Match apparatus	**Length/μm**	**Width/μm**	**Height/μm**	**Normalized flow resistance (R)**	
	17400	150	60	12.6	

Here, the branch channels of the focus structure included two symmetric channels, and we listed the parameters of one branch channel. Similarly, the separation channels included two symmetric channels, and we listed the parameters of one channel. In addition, the five focus structures of the seven groups in focus-separation apparatus were the same, so we listed one group of the focus apparatus. However, the separation channels from the seven groups in focus-separation apparatus were different, as shown in the table. As shown in the table, we normalized the flow resistance (R), and the R of the central channel of the focus structure was set to 1.

Table S2. The Calculated value of focus-separation in the chip.

Focus apparatus	**Separated liquid Width/μm (W-λ_x)**	**Separated liquid ratio (%)**	**Width of cell centroid' boundary from main channel boundary/μm (W-λ^x)**
The first focus structure	14.7	14.3	20.4
The second focus structure	20.3	25.9	24.7
The third focus structure	23.9	34.8	27.0
The fourth focus structure	26.7	42.5	29.7
The fifth focus structure	28.8	48.4	31.4
Separation apparatus	**Separated liquid Width/μm (corresponding to 200 μm width)**	**Separated liquid ratio (%)**	**Converted separated liquid Width/μm (corresponding to 90 μm width)**
The first separation	65.6	49.6	29.2
The second separation	64.9	48.7	28.9
The third separation	64.2	47.9	28.6
The fourth separation	63.9	47.5	28.5
The fifth separation	64.7	48.5	28.8
The sixth separation	62.9	46.1	28.0
The seventh separation	60.9	43.7	27.2

As a result, we can calculate the distribution of the flow among the focus-separation apparatus according to R. For example, the first separation channels separated 49.6% (8.76/(8.76+0.5×17.8=0.496) of the flow. Similarly, the second to the seventh separation channels separated 48.7%, 47.9%, 47.5%, 48.5%, 46.1% and 43.7% (average approximately 47%) of the fluid every time, respectively. We listed the ratio and width of the flow separated by the branch channels and the separation channels in the table. The distribution of 'centroid area' of cancer cells after the focus structures is also listed. At the same time, we listed the separate width of the separation channels corresponding to the channel width of 90 μm, in order to correspond to the distribution of 'centroid area' of cancer cells.

Table S3. Clinical characteristics of the patients used for CTC detection.

Sample number	Cancer type	CTC/mL	Stage
P.1	Breast cancer	117	IV
P.2	Breast cancer	47	IV
P.3	Breast cancer	7	III
P.4	Lung cancer	40	IV
P.5	Lung cancer	30	IV
P.6	Lung cancer	35	III
P.7	Lung cancer	17	IIB
P.8	Liver cancer	7	IV
P.9	Liver cancer	6	IV
P.10	Liver cancer	25	III
P.11	Liver cancer	12	III

Supplementary movie legends

Movies S1 to S3

Movie S1: Video of cancer cells' movement at the 7th focus apparatus using 10× dilution blood at 500 μL/h.

The video played at 0.4x speed. A total of 100,000 RFP-labeled HeLa cells were spiked into 1 mL 10× dilution rabbit blood/ medium, the flow rate was set to 500 μL/h, and the movement of HeLa cells (red fluorescent channel) and blood cells (brightfield) were recorded and merged. HeLa cells (red) gradually focused into the center of the channel.

Movie S2: Video of cancer cells' movement at the 7th separation apparatus using 10× dilution blood under 500 μL/h.

The video played at 2x speed. A total of 100,000 RFP-labeled HeLa cells were spiked into 1 mL 10× dilution rabbit blood/ medium, the flow rate was set to 500 μL/h, and the movement of HeLa cells (red fluorescent channel) and blood cells (brightfield) were recorded and merged. HeLa cells (red) were kept in the main channel, while other blood cells were separated to the outlet by the separation apparatus.

Movie S3: Video of WBCs' movement at the capture apparatus using 2× dilution blood under 40 mL/h.

The video played at 5x speed. A total of 2,000 RFP-labeled HeLa cells were spiked into 1 mL 2× dilution rabbit blood, the blood was pre-stained with Hoechst 33342 (WBCs shown blue), the flow rate was set to 40 mL/h, and the movement of HeLa cells (red fluorescent channel) and WBCs (blue fluorescent channel) were recorded and merged. All HeLa cells were captured in the capture arrays, while most WBCs (blue) flowed out of the chip because of their smaller size and stronger deformation ability.